molecules

MDPI

Article

Structural Characterization and Assessment of Anti-Inflammatory and Anti-Tyrosinase Activities of Polyphenols from *Melastoma normale*

Rui-Jie He [1,2,3], Jun Li [3], Yong-Lin Huang [2,*], Ya-Feng Wang [2], Bing-Yuan Yang [2], Zhang-Bin Liu [2], Li Ge [1], Ke-Di Yang [1,*] and Dian-Peng Li [1,2,*]

[1] School of Chemistry and Chemical Engineering, Guangxi University, Nanning 530004, China; hrj937@gxib.cn (R.-J.H.); geli_2009@163.com (L.G.)
[2] Guangxi Key Laboratory of Functional Phytochemicals Research and Utilization, Guangxi Institute of Botany, Guangxi Zhuang Autonomous Region and Chinese Academy of Sciences, Guilin 541006, China; wyf@gxib.cn (Y.-F.W.); yby@gxib.cn (B.-Y.Y.); lzb@gxib.cn (Z.-B.L.)
[3] State Key Laboratory for the Chemistry and Molecular Engineering of Medicinal Resources, College of Chemistry and Pharmacy, Guangxi Normal University, Guilin 541004, China; lijun9593@gxnu.edu.cn
* Correspondence: hyl@gxib.cn (Y.-L.H.); kdyang@gxu.edu.cn (K.-D.Y.); ldp@gxib.cn (D.-P.L.); Tel.: +86-773-355-0829 (Y.-L.H.); Fax: +86-773-355-0067 (Y.-L.H.)

Citation: He, R.-J.; Li, J.; Huang, Y.-L.; Wang, Y.-F.; Yang, B.-Y.; Liu, Z.-B.; Ge, L.; Yang, K.-D.; Li, D.-P. Structural Characterization and Assessment of Anti-Inflammatory and Anti-Tyrosinase Activities of Polyphenols from *Melastoma normale*. *Molecules* **2021**, *26*, 3913. https://doi.org/10.3390/molecules26133913

Academic Editors: Federica Pellati, Laura Mercolini and Roccaldo Sardella

Received: 13 May 2021
Accepted: 24 June 2021
Published: 26 June 2021

Abstract: Polyphenols, widely distributed in the genus *Melastoma* plants, possess extensive cellular protective effects such as anti-inflammatory, anti-tyrosinase, and anti-obesity, which makes it a potential anti-inflammatory drug or enzyme inhibitor. Therefore, the aim of this study is to screen for the anti-inflammatory and enzyme inhibitory activities of compounds from title plant. Using silica gel, MCI, ODS C18, and Sephadex LH-20 column chromatography, as well as semipreparative HPLC, the extract of *Melastoma normale* roots was separated. Four new ellagitannins, Whiskey tannin C (**1**), 1-*O*-(4-methoxygalloyl)-6-*O*-galloyl-2,3-*O*-(*S*)-hexahydroxydiphenoyl-*β*-D-glucose (**2**), 1-*O*-galloyl-6-*O*-(3-methoxygalloyl)-2,3-*O*-(*S*)-hexahydroxydiphenoyl-*β*-D-glucose (**3**), and 1-*O*-galloyl-6-*O*-vanilloyl-2,3-*O*-(*S*)-hexahydroxydiphenoyl-*β*-D-glucose (**4**), along with eight known polyphenols were firstly obtained from this plant. The structures of all isolates were elucidated by HRMS, NMR, and CD analyses. Using lipopolysaccharide (LPS)-stimulated RAW2 64.7 cells, we investigated the anti-inflammatory activities of compounds **1**–**4**, unfortunately, none of them exhibit inhibit nitric oxide (NO) production, their IC_{50} values are all >50 μM. Anti-tyrosinase activity assays was done by tyrosinase inhibition activity screening model. Compound **1** showed weak tyrosinase inhibitory activity with IC_{50} values of 426.02 ± 11.31 μM. Compounds **2**–**4** displayed moderate tyrosinase inhibitory activities with IC_{50} values in the range of 124.74 ± 3.12–241.41 ± 6.23 μM. The structure–activity relationships indicate that hydroxylation at C-3′, C-4′, and C-3 in the flavones were key to their anti-tyrosinase activities. The successful isolation and structure identification of ellagitannin provide materials for the screening of anti-inflammatory drugs and enzyme inhibitors, and also contribute to the development and utilization of *M. normale*.

Keywords: *Melastoma normale*; *Melastoma*; polyphenols; tyrosinase; anti-inflammatory; ellagitannins

1. Introduction

Inflammation, as a common clinical pathological process, is closely related to many diseases such as arthritis, psychosis, cardiovascular and cerebrovascular diseases, and cancer [1]. Tyrosinase is the key enzyme of melanin synthesis, and its overexpression can lead to pigmentation diseases such as freckles, chloasma and melanoma [2]. At present, anti-inflammatory drugs such as glucocorticoids, insulin, and tyrosinase inhibitors such as kojic acid have been proven to have significant side effects [3,4]. Therefore, finding out the effective and lower side effects anti-inflammatory drugs and tyrosinase inhibitor is of great

importance. Polyphenols, the characteristic component of *Melastoma* plants, have broad cytoprotective effects, such as anti-oxidation, anti-inflammatory, anti-tyrosinase [5], and anti-obesity [6,7], which make it a potential anti-inflammatory drug or enzyme inhibitor. *Melastoma normale* D. Don, a shrub of the Melastomaceae family, is widespread in Nepal, India, Myanmar, Malaysia, Philippines, and China [8]. The roots of *M. normale*, "Yang KaiKou" in Chinese, contain abundant polyphenols, which have been demonstrated as bioactive constituents corresponding to the anti-inflammatory effect of this plant [9–11]. With the aim to screen for the anti-inflammatory and enzyme inhibitory activities of compounds from the title plant, the roots of *M. normale* were extracted by 80% aqueous acetone and subsequent separated by various chromatographic methods to yield twelve polyphenols. The structures of the isolates were characterized by comprehensive spectroscopic data analyses. Moreover, the anti-inflammatory activities of new compounds **1**–**4** were investigated to develop Polyphenols as a novel anti-inflammatory drug. In addition, anti-tyrosinase activities of compounds **1**–**12** were evaluated, and the structure–activity relationships of compounds **7**–**12** were studied. In this study, there are five ellagitannins were isolated from *M. normale*. As we all known, ellagitannin is esters of hexahydroxydiphenoic acid and monosaccharide. The separation of these compounds is often difficulty due to its high polarity, easy to be adsorbed by separation materials, and unstable to light and heat. Moreover, because of its large molecular weight, many identical structural units in the structure, as well as the serious overlap of NMR, the determination of its structure has always been a difficult problem. Therefore, separation and structural identification of these compounds is still a difficult problem in the field of natural product chemistry. The successful isolation and structural identification of the ellagitannins provide materials for this experiment, and also contribute to the development and utilization of the plant.

2. Results and Discussion

The EtOAc fraction of the 80% aqueous acetone extract of *M. normale* roots was purified using various chromatographic methods to give four new compounds **1**–**4** and eight known compounds **5**–**12**. The structures of **1**–**12** are shown in Scheme 1. The known compounds **5**–**12** were identified as mongolicain A (**5**) [12], 1-hydroxy-3,4,5-trimethoxy phenyl-1-*O*-[6′-*O*-(4″-carboxy-1″,3″,5″-trihydroxy)phenyl]-*β*-D-glucopyranoside (**6**) [13], kaempferol (**7**) [14], kaempferol-3-rhamnoside (**8**) [15], gentisic acid-5-*O*-*β*-D-(6′-*O*-galloyl)-glucopyranside (**9**) [16], quercetin (**10**) [17], quercetin-3-*O*-*α*-L-rhamnoside (**11**) [18], and myricetin-3-*O*-*α*-L-rhamnopyranoside (**12**) [19], respectively. All compounds were firstly isolated from this plant. Moreover, the ellagitannins are firstly obtained from the roots of *M. normale* [10,11,20].

2.1. Structure Elucidation

Compound **1** was obtained as a yellow amorphous powder and showed the positive a coloration characteristic of ellagitannins with the $NaNO_2$-AcOH reagent. The molecular formula $C_{45}H_{34}O_{27}$ was established by the HRESIMS spectrum with a negative-ion peak at m/z $[M - H]^-$ 1005.1240 (calcd 1005.1215). The ^{1}H-NMR data (Table 1) revealed at least two hexahydroxydiphenoyl (HHDP) groups (δ 6.60, 6.70, and 6.83), six methine groups, three oxygen-bearing methylene groups, and two methyl groups. The ^{13}C NMR data (Table 1) revealed six ester carbonyl groups at δ 170.5, 170.1, 168.9, 168.8, 167.6, and 163.3. The presence of two ethoxyls was indicated by the ^{1}H-^{1}H COSY correlations (Figure 1). The NMR data (Table 1) and ^{1}H-^{1}H COSY correlations (Figure 1) revealed a polyalchohol unit, which was similar to the open-chain glucose unit of vescalagin [21]. The relatively lowfield carbon chemical shifts of the glucose C-2–C-6 and HMBC correlations (Figure 1) indicated that hydroxyl groups at the glucose C-2–C-6 were acylated. One of the two HHDP groups attached to the glucose C-4 and C-6 was confirmed by a large difference the chemical shifts between the H-6a (δ 4.95) and H-6b (δ 3.95) [22], and HMBC correlations of the glucose H-4 and H-6 with the carbonyl carbons $C_{HHDP\text{-}7'}$ (δ 168.9) and $C_{HHDP\text{-}7'''}$ (δ 170.1), respectively. A cyclopentenone ring possessing an ethoxycarbonyl

group could be constructed by analysis of the carbon signals due to a carbonyl (δ 202.9 (Cp-3)), an ester carbonyl (δ 170.5 (Cp-7)), two olefinic (δ 143.8 (Cp-4) and 158.2 (Cp-5)), a methine (δ 46.3 (Cp-1)), and an oxygen-bearing quaternary carbon (δ 84.9, Cp-2). This was supported by the HMBC correlations of methylene protons (δ 4.25) with Cp-7 and H_{Cp}-1 (δ 5.46) with Cp-2, Cp-3, Cp-4, Cp-5, and Cp-7. In addition, the connection of the Cp-4 to the glucose C-1 was demonstrated by the HMBC correlations of the glucose H-1 with Cp-3, Cp-4, and Cp-5. The relatively high-field ester carbonyl carbon chemical shift at δ 163.3 (Cp-6) suggested that this carbonyl was linked to a double bond and form a δ-lactone ring with the glucose C-2 hydroxyl group. This was confirmed by HMBC correlation of the ester carbonyl carbon (δ 163.3) with glucose H-2. The correlations of H_{Cp}-1 with C_{HHDP-2} (δ 125.0), C_{HHDP-3} (δ 111.2), and C_{HHDP-4} (δ 146.4) in the HMBC spectrum (Figure 1) indicated that Cp-1 was conjugated with C_{HHDP-3}. Moreover, the glucose C-3 and C-5 hydroxyl groups formed other two lactone rings with two carbonyl groups attached to the hexahydroxybiphenyl moiety. This was demonstrated by the HMBC correlations of glucose H-3 with ester carbonyl carbon (C_{HHDP-7} δ 167.6) and the glucose H-5 and the aromatic proton $H_{HHDP-3'}$ with ester carbonyl carbon ($C_{HHDP-7'}$ δ 168.9). The key HMBC correlations of the methylene protons (δ 3.60 and 3.52) with the glucose C-1 (δ 68.0) and the glucose H-1 (δ 4.34) with the methylene carbon (δ 66.0) indicated that the ethoxyl moiety was located at the glucose C-1. Therefore, the 2D structure of **1** was established. This was supported by comparing the spectroscopic data of **1** with those of Whiskey tannin B [23]. The small coupling constant between glucose H-1 and H-2 (J < 2.0 Hz) revealed that the configuration at glucose C-1 of **1** was the same as that of vescalagin (J = 2.0 Hz) [21], and different from that of Whiskey tannin B (J = 6.4 Hz) [23]. Assuming that **1** was derived from vescalagin, construction of a Dreiding model of **1** indicated that the benzyl methine proton (Cp-1) of the cyclopentenone ring must be β-configuration, because its fused ring system, including two aromatic rings, a cyclopentene, and 6- and 10-membered lactone rings, was so rigid that an alternative model could not be constructed. The absence of ROE correlations between the Cp-1 proton and the methoxyl group suggested an α-orientation of the ethoxycarbonyl group. The CD spectrum of **1** (Figure S26) showed a positive Cotton effect at 240 nm and a negative one at 263 nm indicating that the atropisomerism of the HHDP group had the *S*-configuration [24]. Based on these results, the structure of compound **1**, named Whiskey tannin C, was established as depicted in Scheme 1.

Table 1. ^{1}H (500 MHz) and ^{13}C-NMR (125 MHz) Spectroscopic Data for **1** in Methanol-d_4.

Pos.	δ_C	δ_H	Pos.	δ_C	δ_H	Pos.	δ_C	δ_H
Glc-1	68.0	4.34 d (0.9)	HHDP-1	114.4		HHDP-1″	116.6	
2	80.6	5.11 d (0.9)	2	125.0		2″	125.0	
3	70.0	5.48 d (7.5)	3	111.2		3″	108.6	6.83 s
4	70.5	5.48 d (7.5)	4	146.4		4″	145.3	
5	71.5	5.39 m	5	136.4		5″	138.2	
6a	65.7	4.95 overlapped	6	146.8		6″	146.5	
6b		3.95 dd (12.8, 2.5)	7	167.6		7″	168.8	
Cp-1	46.3	5.46 s	HHDP-1′	114.6		HHDP-1‴	116.0	
2	84.9		2′	125.0		2‴	126.5	
3	202.9		3′	108.6	6.70 s	3‴	108.0	6.60 s
4	143.8		4′	145.0		4‴	145.4	
5	158.2		5′	138.0		5‴	138.0	
6	163.3		6′	146.0		6‴	145.9	
7	170.5		7′	168.9		7‴	170.1	
OCH_2	63.8	4.25 q (7.1)	OCH_2	66.0	3.60 m; 3.52 m			
CH_3	14.3	1.24 t (7.1)	CH_3	15.5	1.16 t (7.0)			

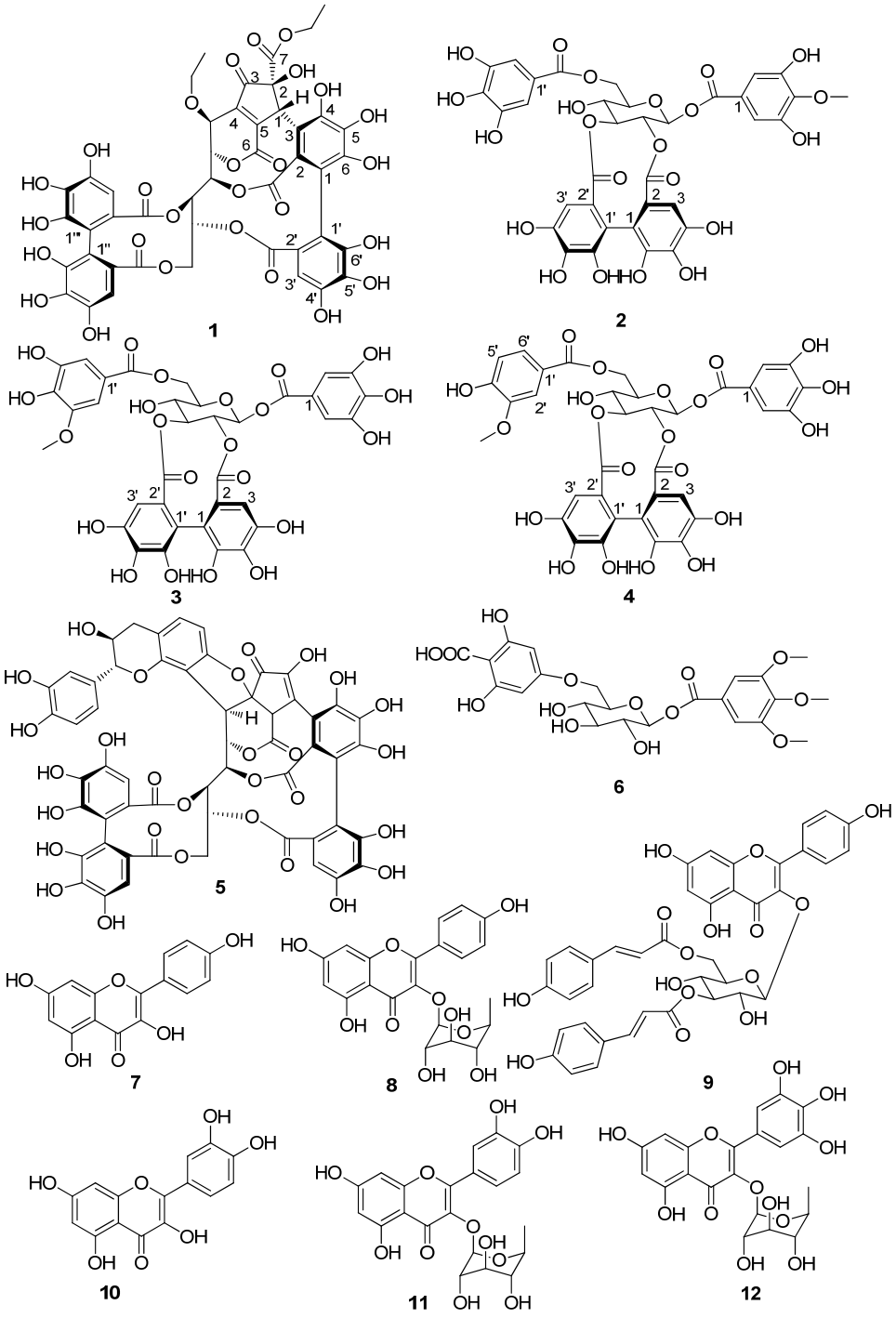

Scheme 1. Structures of compounds **1**–**12**.

Compound **2** was isolated as a brown amorphous powder. The molecular formula $C_{35}H_{28}O_{22}$ was determined based on the $[M - H]^-$ peak at m/z 799.0983 (calcd 799.0999) in its HRESIMS spectrum. The ^{1}H NMR data (Table 2) revealed two galloyl groups (δ_H 7.12 (2H, s) and 7.11 (2H, s)), an HHDP group (δ_H 6.72 (1H, s) and 6.43 (1H, s)), and a methoxyl group (δ_H 3.87 (3H, s)). The relatively low-field chemical shifts and the relatively large coupling patterns of the sugar protons indicated that glucose cores in **2** adopt the $^4C_1$ conformation and the acyl groups should be located at *O*-1, *O*-2, *O*-3, and *O*-6. The location of the HHDP group at glucose *O*-2/*O*-3 was supported by evidence from the HMBC correlations, the ^{1}H-^{1}H COSY correlations (Figure 2), as well as the chemical shift (δ 92.6) of the anomeric carbon signals [25]. The (*S*) configuration of the HHDP group was

confirmed by the CD spectrum, which exhibited a positive cotton effect at 238 nm and a negative cotton effect at 264 nm [24]. The coupling constant of the anomeric proton in **2** was 8.5 Hz, indicating that the sugar moiety had a *β* configuration. Comparison of its NMR data (Table 2) with those of 1,6-di-*O*-galloyl-2,3-*O*-(*S*)-hexahydroxydiphenoyl-*β*-D-glucose [20] revealed that the hydroxy group at galloyl-C-4 in the latter was replaced by a methoxyl group in the former. The molecular formula, the chemical shifts of galloyl-C-3 (δ_C 151.5), galloyl-C-4 (δ_C 141.3), galloyl-C-5 (δ_C 151.5), and -OCH_3 (δ_C 60.8), and the correlations of aromatic proton (δ_H 7.12) and methoxyl proton (δ_H 3.87) with galloyl-C-4 (δ_C 141.3) in the HMBC spectrum supported these changes in **2**. Acid hydrolysis and subsequent methylation and silylation of **2** established that the sugar in the molecule was D-glucose. The structure of **2** was therefore established as 1-*O*-(4-methoxygalloyl)-6-*O*-galloyl-2,3-*O*-(*S*)-hexahydroxydiphenoyl-*β*-D-glucose.

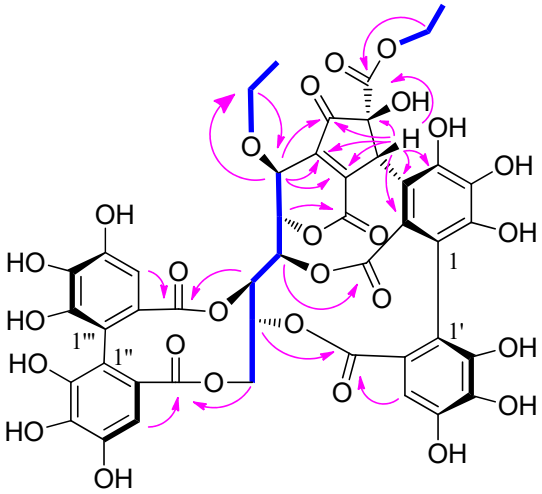

Figure 1. Key HMBC (arrows) and ^{1}H-^{1}H COSY (bonds) correlations of **1**.

Compound **3** had the same molecular formula as compound **2**, as determined by its HRESIMS data. Comparison between the NMR data of **3** and **2** (Table 2) revealed that the methoxyl group at galloyl-C-4 in **2** shifted to galloyl-C-3′ in **3**. This was confirmed by the HMBC correlations (Figure 2) of the methoxyl protons (δ_H 3.88) and aromatic proton (δ_H 7.24) with galloyl-C-3′ (δ_C 149.1) in **3**, and the chemical shifts of the methoxyl group, galloyl-C-3, galloyl-C-4, and galloyl-C-3′ that shifted from δ_C 60.8, 151.5, 141.3, and 146.5 in **2** to δ_C 56.7, 146.6, 140.7, and 149.1 in **3**, respectively. A positive cotton effect at 237 nm and a negative one at 262 nm in the CD spectrum indicated the (*S*) configuration of the HHDP group for **3** [24]. The *β* configuration of the sugar moiety was deduced from the coupling constant (J = 8.5 Hz) of the anomeric proton of the glucosyl moiety. Acid hydrolysis of **3** with 1 M HCl yielded D-glucose, which was confirmed by TLC and GC analyses. Hence, compound **3** was identified as 1-*O*-galloyl-6-*O*-(3-methoxygalloyl)-2,3-*O*-(*S*)-hexahydroxydiphenoyl-*β*-D-glucose.

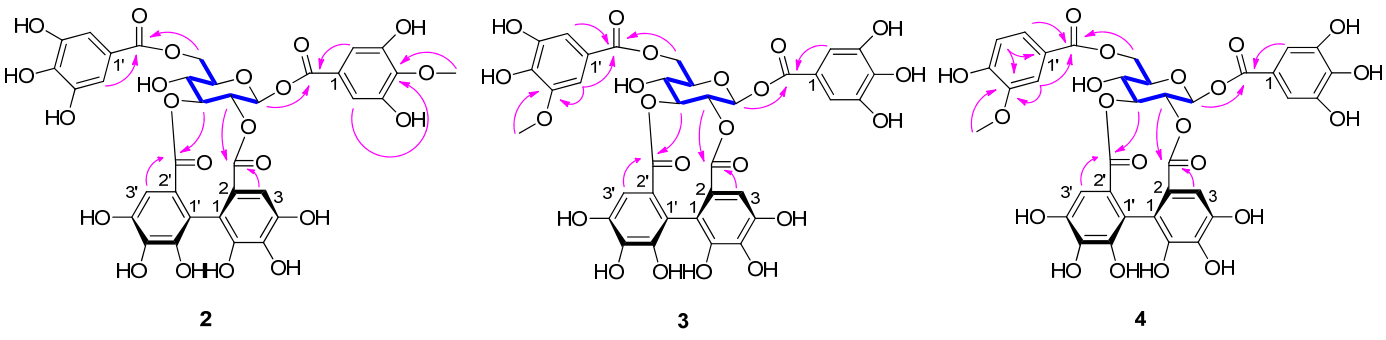

Figure 2. Key HMBC (arrows) and ^{1}H-^{1}H COSY (bonds) correlations of **2**–**4**.

Table 2. ^{1}H (500 MHz) and ^{13}C NMR (125 MHz) Spectroscopic Data for **1** in Methanol-d_4.

	2		**3**		**4**	
Pos.	δ_C	δ_H	δ_C	δ_H	δ_C	δ_H
Glc-1	92.6	6.15 d (8.5)	92.6	6.13 d (8.5)	92.6	6.13 d (8.5)
2	75.9	5.12 dd (8.5, 9.7)	75.9	5.12 m	75.8	5.12 dd (8.5, 9.5)
3	80.5	5.27 d (9.7)	80.6	5.25 d (9.6)	80.6	5.26 d (9.4)
4	68.1	4.00 d (9.7)	68.5	3.95 d (9.6)	68.6	3.95 d (9.4)
5	76.6	4.03 dd (5.8, 2.1)	76.8	3.99 m	76.8	4.00 dd (5.8, 2.1)
6a	64.1	4.64 d (11.9)	64.2	4.69 d (11.0)	64.3	4.73 d (12.0)
6b		4.53 dd (11.9, 3.7)	-	4.45 m	-	4.46 dd (12.0, 5.8)
galloyl-1	119.7	-	119.8	-	119.8	-
2	110.3	7.12 s	110.5	7.10 s	110.4	7.11 s
3	151.5	-	146.6	-	146.6	-
4	141.3	-	140.7	-	140.7	-
5	151.5	-	146.6	-	146.6	-
6	110.3	7.12 s	110.5	7.10 s	110.4	7.11 s
COO-	166.2	-	166.2	-	166.1	-
galloyl/vanilloyl-1′	122.2	-	121.1	-	122.2	-
2′	110.4	7.11 s	106.3	7.24 d (1.7)	113.6	7.57d (1.8)
3′	146.5	-	149.1	-	148.7	-
4′	140.7	-	140.7	-	152.8	-
5′	146.5	-	145.8	-	115.9	6.87 d (8.3)
6′	110.4	7.11 s	111.9	7.22 d (1.7)	125.2	7.60 dd (8.3, 1.8)
COO-	167.7	-	168.0	-	167.9	-
HHDP-1	115.2	-	115.3	-	115.3	-
2	126.1	-	126.1	-	126.1	-
3	107.4	6.43 s	107.5	6.43 s	107.5	6.43 s
4	145.7	-	144.9	-	144.9	-
5	137.3	-	137.4	-	137. 4	-
6	144.8	-	146.5	-	145.7	-
COO-	170.2	-	170.2	-	170.2	-
HHDP-1′	115.3	-	115.4	-	115.4	-
2′	126.1	-	126.6	-	126.6	-
3′	107.9	6.72 s	107.9	6.70 s	107.9	6.71 s
4′	144.7	-	144.8	-	144.8	-
5′	137.4	-	137.5	-	137.5	-
6′	145.7	-	146.1	-	145.8	-
COO-	171.0	-	171.0	-	171.0	-
CH_3O-	60.8	3.87 s	56.7	3.88 s	56.4	3.90 s

The molecular formula of **4** was deduced from its HRESIMS spectrum (*m*/*z* 783.1032, $[M - H]^-$) as C_{35} H_{28} O_{21}. Its molecular weight was 16 mass units less than that of **3**, which may be attributed to the absence of a hydroxyl and the presence of an aromatic proton (δ_H 6.87) at vanilloyl-C-5′ in **4** (Table 2). This was confirmed from the presence of a 1,2,4-trisubstituted aromatic moiety (δ_H 7.60 (dd, *J* = 8.3, 1.8 Hz), 6.87 (d, *J* = 8.3 Hz), and 7.57 (d, *J* = 1.8 Hz)) and the chemical shift change of galloyl-C-5′ at δ_C 145.8 in **3** to vanilloyl-C-5′ at δ_C 115.9 in **4**. The methoxyl protons (δ_H 3.90) and aromatic proton (δ_H 6.87) correlations with vanilloyl-C-3′ in the HMBC spectrum (Figure 2) further confirmed the aromatic proton (δ_H 6.87) at vanilloyl-C-5′. The atropisomerism of the HHDP was shown to be an *S* configuration by appearance of positive and negative cotton effects at 239 nm and 263 nm, respectively [24]. The coupling constants of the anomeric proton in **4** were 8.5 Hz reminiscent of *β*-anomeric configuration. The acid hydrolysis revealed that **4** had the same sugar units as **3**. Thus, compound **4** was identified as 1-*O*-galloyl-6-*O*-vanilloyl-2,3-*O*-(*S*)-hexahydroxydiphenoyl-*β*-D-glucose.

2.2. Anti-Inflammatory Activity Assays

Four new compounds **1**–**4** were tested for potential anti-inflammatory activity by measuring the inhibition of the nitric oxide (NO) production. Unfortunately, none of them displayed significantly anti-inflammatory activity. The IC_{50} values for the inhibition of NO production by compounds **1**–**4** are all > 50 μM. It has been reported that the known flavonols kaempferol (**7**) [26], quercetin (**10**) [27], and myricetin-3-*O*-*α*-L–rhamnopyranoside (**12**) [28] have anti-inflammatory activity, but kaempferol-3-rhamnoside (**8**) [26] and quercetin-3-*O*-

α-L-rhamnoside (**11**) [29] have no anti-inflammatory activity. From the experimental results and literature data, the flavonoids in the title plant have better anti-inflammatory activity than ellagitannins, it may be the active ingredient corresponding to the anti-inflammatory effect of this plant.

2.3. Tyrosinase Inhibitory Activity Assays

All compounds were investigated for potential tyrosinase inhibitory activity. As shown in Table 3, new compounds **2**–**4** displayed moderate tyrosinase inhibitory activities. New compound **1** exhibited weak tyrosinase inhibitory activity. Quercetin (**10**) [30] has a significant tyrosinase inhibitory activity, and its anti-tyrosinase activity is better than quercetin-3-*O*-α-L-rhamnoside (**11**) [26] and kaempferol (**7**) [26], which is consistent with the literature data. This indicated that 3′- and 4′-hydroxy groups on the B ring and 3-hydroxy group on the C ring in flavonols were crucial to their activities. The anti-tyrosinase activity of kaempferol (**7**) [26] is better than kaempferol-3-rhamnoside (**8**) [26], and compounds **8** and **12** [31] has no significant anti-tyrosinase activity, which further supports the above structure–activity relationships.

Table 3. Tyrosinase inhibitory activity of isolates **1**–**12** ($IC_{50} \pm SD$, μM).

Compound	IC_{50} (μM)	Compound	IC_{50} (μM)
1	426.02 ± 11.31	**8**	>2000.00
2	241.41 ± 6.23	**9**	421.23 ± 10.63
3	153.54 ± 3.63	**10**	76.83 ± 2.02
4	124.74 ± 3.12	**11**	98.24 ± 2.31
5	361.92 ± 8.81	**12**	904.93 ± 20.42
6	357.83 ± 9.22	kojic acid	100.52 ± 2.63
7	1899.34 ± 38.21		

3. Experimental

3.1. Materials

The roots of *M. normale* were collected from Yanshan Town, Guilin City, Guangxi Province, in September 2018, and authenticated by Professor Yusong Huang (Guangxi Institute of Botany). A voucher specimen (20180912) was deposited in the Guangxi Key Laboratory of Functional Phytochemicals Research and Utilization, Guangxi Institute of Botany, China.

3.2. General Experimental Procedures

Optical rotations were measured with an ADP440+ polarimeter (λ 589 nm, path length 1.0 cm). The NMR spectra were acquired on a Bruker Advance 500 spectrometer (Bruker Biospin AG, Fällanden, Switzerland), and the residual solvent peaks were used as references. Coupling constants and chemical shifts were given in Hz and on a δ (ppm) scale, respectively. The ESIMS and HRESIMS data were recorded on a BRUKER HCT mass spectrometer and LCMS-IT-TOF spectrometer (Shimadzu, Kyoto, Japan), respectively. GC was performed on an Agilent 7890N (Agilent Technologies, Inc. Chandler, AZ, USA) system with a 0.32 mm i.d. × 25 m L-Chirasil-Val column. Analytical HPLC was run on a Shimadzu LC-2030C HPLC (Shimadzu, Kyoto, Japan) system using a 4.6 i.d. × 250 mm Agilent Eclipse XDB-C_{18} (5 μm) column. Semi-preparative HPLC was conducted on a Shimadzu LC-20AT HPLC system using a 20.0 i.d. × 250 mm Dr. Maisch reprosil 100 C18 (5 μm) column at a flow rate of 4 mL/min. Column chromatography (CC) was performed using Sephadex LH-20 (25–100 μm; GE Healthcare Bio-Science AB, Uppsala, Sweden), silica gel column (200–300 mesh, Qingdao Marine Chemical Co. Ltd., Qingdao, China), MCI gel CHP 20P (75–150 μm; Mitsubishi Chemical Co., Tokyo, Japan), and Chromatorex ODS (50 μm, Merck, Darmstadt, Germany) columns.

3.3. Extraction and Separation

Air-dried, powdered roots (10 kg) of *M. normale* were extracted with 80% aqueous acetone (3 × 7 days) at room temperature and each extract filtered. The filtrates were dried under reduced pressure to afford a crude extract (0.6 kg). The extract was suspended in H_2O (1 L) and successively partitioned with petroleum ether (3 × 2 L), EtOAc (3 × 2 L). The EtOAc extract (80 g) was divided into ten fractions (Fr.1–10) by silica gel CC (8 i.d. × 20 cm) eluting with a gradient of CH_2Cl_2-MeOH (100:0, 95:5, 90:10, 80:20, 70:30, 50:50, 0:100, *v*/*v*). Fr.4 (32 g) was loaded onto an MCI gel column (6 i.d. × 20 cm) and eluted with a gradient of MeOH-H_2O (0:100–100:0, *v*/*v*) to afford eighteen subfractions (Fr 4-1–4-18). Separation of subfraction Fr 4-14 (3.0 g) was done by another silica gel column (3 i.d. × 20 cm) eluting with a gradient of CH_2Cl_2-MeOH (97:3–80:20, *v*/*v*) and Sephadex LH-20 CC eluting with CH_2Cl_2-MeOH (1:1, *v*/*v*) to afford **7** (11.3 mg), **8** (10.6 mg), **9** (9.3 mg), **10** (20.6 mg), **11** (7.6 mg), and **12** (6.2 mg). Fr 6 (4.2 g) was applied to ODS C18 column and eluted with MeOH-H_2O (20:80–80:20) to obtain 9 subfractions (Fr 6-1–6-9). Further separation of subfraction Fr 6-4 (1.2 g) using Sephadex LH-20 CC (eluted with MeOH-H_2O, 10:90–100:0) yielded compounds **1** (9.6 mg), **5** (7.2 mg), and **6** (7.3 mg), respectively. Compounds **2** (t_R 130.5 min, 5.2 mg), **3** (t_R 146.8 min, 9.6 mg), and **4** (t_R 177.2 min, 15.3 mg) were obtained from Fr 7 (2.5 g) via semipreparative HPLC eluting with a gradient of MeOH-H_2O (20:80–40:60, *v*/*v*, 0–250 min).

3.4. Spectroscopic Data

Whiskey tannin C (**1**): Brown amorphous powder; $[\alpha]_D^{25}$ −12.6° (*c* = 0.16, MeOH); UV (MeOH) λ_{max} nm (log ε): 203 (2.02), 276 (1.19); CD (MeOH) λ_{max} ($\Delta\varepsilon$) 263 (−7.8), 240 (10.9), 225 (2.9). ^{1}H and ^{13}C NMR data, see Table 1; HRESIMS *m*/*z*: $[M - H]^-$ 1005.1240 (calcd for $C_{45}H_{33}O_{27}^-$, 1005.1215).

*1-O-(4-methoxygalloyl)-6-O-galloyl-2,3-O-(S)-hexahydroxydiphenoyl-β-*D*-glucose* (**2**): Brown amorphous powder amorphous powder; $[\alpha]_D^{25}$ −5.5° (*c* = 0.17, MeOH); UV (MeOH) λ_{max} nm (log ε): 203 (2.52), 275 (2.01); CD (MeOH) λ_{max} ($\Delta\varepsilon$) 264 (−8.0), 238 (30.6), 218 (1.3). ^{1}H and ^{13}C-NMR data, see Table 2; HRESIMS *m*/*z*: 799.0983 $[M - H]^-$ (calcd for $C_{35}H_{27}O_{22}^-$, 799.0999).

*1-O-galloyl-6-O-(3-methoxygalloyl)-2,3-O-(S)-hexahydroxydiphenoyl-β-*D*-glucose* (**3**): Brown amorphous powder; $[\alpha]_D^{25}$ −33.5° (*c* = 0.12, MeOH); UV (MeOH) λ_{max} nm (log ε): 203 (2.40), 273 (1.68); CD (MeOH) λ_{max} ($\Delta\varepsilon$) 262 (−3.1), 237 (11.1), 210 (−2.7). ^{1}H and ^{13}CNMR data, see Table 2; HRESIMS *m*/*z*: 799.1006 $[M - H]^-$ (calcd for $C_{35}H_{27}O_{22}^-$, 799.0999).

*1-O-galloyl-6-O-vanilloyl-2,3-O-(S)-hexahydroxydiphenoyl-β-*D*-glucose* (**4**): Brown amorphous powder; $[\alpha]_D^{25}$ −20.6° (*c* = 0.15, MeOH); UV (MeOH) λ_{max} nm (log ε): 203 (2.42), 278 (1.86); CD (MeOH) λ_{max} ($\Delta\varepsilon$) 263 (−12.1), 239 (42.5), 219 (0.9). ^{1}H and ^{13}CNMR data, see Table 2; HRESIMS *m*/*z*: 783.1032 $[M - H]^-$ (calcd for $C_{35}H_{27}O_{21}^-$, 783.1050).

3.5. Acid Hydrolysis of **2**–**4**

Compound **2** (2 mg) was treated with 1 M HCl (5 mL) at 80 °C for 4 h, and then extracted with ethyl acetate (3 × 5 mL). The aqueous phase was dried under a stream of N_2 to generate a neutral residue that was analysed using TLC (SiO_2) with EtOAc-pyridine-EtOH-H_2O (7:1:1:2) as solvent system. The R_f value of the neutral residue was the same as that of authentic D-glucose indicated the sugar component of 2 was glucose. The neutral residue and 5 mg L-cysteine methyl ester hydrochloride were dissolved successively in 3 mL of anhydrous pyridine and warmed at 80 °C for 1 h. After removal of the solvent by evaporation under reduced pressure, the reaction mixture was subsequently reacted with 0.6 mL of N-trimethylsilylimidazole at 80 °C for 1 h. The reaction mixture was partitioned with n-hexane and H_2O, and then the n-hexane layer was analysed by a GC instrument. The injector and detector temperatures were set at 250 °C and 280 °C, respectively. The initial column temperature was held at 160 °C for 1 min, then increased to 280 °C at 5 °C/min. and held for 10 min. The authentic D-glucose and authentic L-glucose were

silylated and analyzed in the same way, and their retention times were 19.09 and 19.25 min, respectively. The results of the GC analysis indicated that the sugar component of **2** was D-glucose (t_R 19.1 min). The sugar components of **3** and **4** were determined using the same procedure.

3.6. Anti-Inflammatory Activity

3.6.1. NO Production by LPS-Stimulated RAW 264.7 Cells

The RAW 264.7 cells were cultivated in DMEM supplemented with 10% FBS at 37 °C in a humidified atmosphere of 5% CO_2 for 24 h. Cells in 24-well plate (5×10^4 cells/well) were treated with 200 ng/mL LPS and the test compounds. After 22 h, the media were collected, and the level of nitrite was measured using the Griess Reagent System (Promega, Madison, WI, USA).

3.6.2. Cell Viability

MTT assay was carried out to measure cytotoxicity of test samples on the RAW264.7 cell line. Cells which were in logarithmic growth phase were seeded in 96-well plate at the density of 5×10^4–6×10^4 cells/well and incubated at 37 °C with 5% CO_2 for 24 h. Next, the cells were treated with 100 µL of culture medium at various concentrations of test samples for 24 h. The medium was discarded and 100 µL of FBS free medium containing MTT (1 mg/mL) was added to each well. After incubation in the incubator for 4 h, the supernatant was discarded and 100 µL of DMSO was added to each well to dissolve the formazan. The absorbance was measured at 570 nm using a microplate reader.

$$\text{Cell viability (\%)} = (\text{absorbance of sample/absorbance of control}) \times 100$$

3.7. Anti-Tyrosinase Activity

The anti-tyrosinase activities of the isolates were investigated according to the procedure described by Aoki et al. with slight modifications [21]. L-DOPA and kojic acid were used as substrate and positive control, respectively. Solution of L-DOPA at 5.0 mM, mushroom tyrosinase at 100 U/mL, as well as samples at different concentrations were prepared in phosphate buffer (pH 6.8). 20 µL of the sample solution and 10 µL of mushroom tyrosinase solution were mixed and pre-incubated at 37 °C for 10 min, then 40 µL of L-DOPA solution was added and incubated at 37 °C for 5 min. The reaction system of anti-tyrosinase activity experiment is shown in Table 4. The absorbance was measured at 475 nm using the Spark 10M multimode microplate reader (Tecan Trading AG, Zurich, Switzerland). All assays were repeated three times and each time in triplicate. The percent inhibition of tyrosinase activity was calculated using the following formula:

$$\text{Tyrosinase inhibition (\%)} = [1 - (T - T_0)/(C - C_0)] \times 100$$

where T represents the absorbance with sample and tyrosinase; T_0 represents the absorbance with sample but no tyrosinase; C represents the absorbance with tyrosinase but no sample; C_0 represents the absorbance without tyrosinase and sample.

Table 4. Reaction system of tyrosinase inhibition activity experiment.

Reagent	T-Sample Tube	T_0-Sample Background	C-DPPH Tube	C_0-Solvent Background
sample	20 µL	20 µL	——	——
pbs	——	10 µL	20 µL	30 µL
tyrosinase	10 µL	——	10 µL	——
L-DOPA	40 µL	40 µL	40 µL	40 µL

4. Conclusions

The study is intended to explore more anti-inflammatory and enzyme inhibitory activities of polyphenols from the roots of *M. normale* on the basis of our previous works [20]. As expected, twelve polyphenols were obtained from the tile plant for the first time, and compounds **1**–**4** were new ellagitannin. The successful isolation and structure identification of ellagitannin provide materials for the screening of anti-inflammatory drugs and enzyme inhibitors, and also contribute to the development and utilization of *M. normale*. Ellagitannins **1**–**4** have no significant tyrosinase inhibitory activities and anti-inflammatory activities, which makes it less likely to be a potential anti-inflammatory drug or enzyme inhibitor. Fortunately, they possess new effects, such as anti-obesity [6,7]. Flavonoids have better anti-inflammatory and inhibitory enzyme activities than ellagitannins in the roots of *M. normale*, and they are more likely to be anti-inflammatory and anti-enzyme inhibitor. The study of structure–activity relationship is helpful to find new anti-inflammatory drugs and enzyme inhibitors.

Supplementary Materials: The following are available online, Figures S1–S6: 1D and 2D NMR spectra of **1**, Figure S7: HRESIMS spectrum of **1**; Figures S8–S12: 1D and 2D NMR spectra of **2**, Figure S13: HRESIMS spectrum of **2**; Figures S14–S18: 1D and 2D NMR spectra of **3**, Figure S19: HRESIMS spectrum of **3**; Figures S20–S24: 1D and 2D NMR spectra of **4**, Figure S25: HRESIMS spectrum of **4**; and Figure S26: CD spectra of **1**–**4**.

Author Contributions: Conceptualization, R.-J.H.; methodology, Y.-L.H. and D.-P.L.; software, R.-J.H.; validation, R.-J.H., Y.-L.H. and D.-P.L.; formal analysis, R.-J.H. and J.L.; investigation, Y.-F.W., B.-Y.Y. and Z.-B.L.; resources, Y.-L.H. and D.-P.L.; data curation, J.L., L.G. and K.-D.Y.; writing—original draft preparation, R.-J.H.; writing—review and editing, R.-J.H.; visualization, R.-J.H.; supervision, K.-D.Y., Y.-L.H. and D.-P.L.; project administration, Y.-L.H.; funding acquisition, Y.-L.H. All authors have read and agreed to the published version of the manuscript.

Funding: This work was supported by the National Natural Science Foundation of China (32060108; 82060764); the Natural Science Foundation of Guangxi (2018GXNSFAA294033; 2018 GXNSFAA281078); The China Postdoctoral Science Foundation (200626); Fundamental Research Fund of Guangxi Institute of Botany (GUIZHIYE 18004); Guangxi Innovation-Driven Development Special Fund (GuiKe AA18118015); the Guangxi Key Laboratory of Functional Phytochemicals Research and Utilization of Open Fund Project (ZRJJ2018-19; ZRJJ2020-2); State Key Laboratory for the Chemistry and Molecular Engineering of Medicinal Resources, Guangxi Normal University (CMEMR2019-B13); Key-Area Research and Development Program of Guangdong Province (2020B1111110003); and Special project of central government guiding local science and technology development (GUIKE 20111010).

Conflicts of Interest: The authors declare no conflict of interest.

Sample Availability: Samples of **1**–**12** are available from the authors.

References

1. Alexander, A.; Maurya, J.; Swarna, S. Various aspects of inflammation and the herbal drugs that are used for the treatment of inflammation: An overview. *J. Pharm. Res.* **2011**, *6*, 1598–1600.
2. Qu, L.; Song, K.; Zhang, Q.; Guo, J.; Huang, J. Simultaneous determination of six isoflavones from puerariae lobatae radix by cpe-hplc and effect of puerarin on tyrosinase activity. *Molecules* **2020**, *25*, 344. [CrossRef]
3. Mariana, L.D.F.; Freitas, M.D.M.; Maria, C.S.C.; Mariela, M.A.E.S. Effect of glucocorticoids on glyceroneogenesis in adipose tissue: A systematic review. *Biochimie* **2020**, *168*, 210–219.
4. Burnett, C.L.; Bergfeld, W.F.; Belsito, D.V. Final report of the safety assessment of kojic acid as used in cosmetics. *Int. J. Toxicol.* **2010**, *29*, 187–213. [CrossRef]
5. Zou, Z.; Shou, X.Y.; Min, J.G.; Zhou, Y.L.; Liu, H.G.; Zou, J.M. Determination of gallic acid and ellagic acid in Zhuang Medicine radix and rhizome of Melastomus normale by HPLC. *Chin. Trad. Herb. Drugs* **2012**, *43*, 2206–2208.
6. Illesca, P.; Valenzuela, R.; Espinosa, A.; Echeverría, F.; Soto-Alarcon, S.; Ortiz, M.; Videla, L.A. Hydroxytyrosol supplementation ameliorates the metabolic disturbances in white adipose tissue from mice fed a high-fat diet through recovery of transcription factors Nrf2, SREBP-1c, PPAR-γ and NF-κB. *Biomed. Pharmacother.* **2019**, *109*, 2472–2481. [CrossRef]

7. Valenzuela, R.; Illesca, P.; Echeverría, F.; Espinosa, A.; Rincón-Cervera, M.Á.; Ortiz, M.; Hernandez-Rodas, M.C.; Valenzuela, A.; Videla, L. Molecular adaptations underlying the beneficial effects of hydroxytyrosol in the pathogenic alterations induced by a high-fat diet in mouse liver: PPAR-alpha and Nrf2 activation, and NF-kappaB down-regulation. *Food Funct.* **2017**, *8*, 1526–1537. [CrossRef] [PubMed]
8. Editorial Committee of the Flora of China of Chinese Academy of Sciences. *Flora Reipublicae Popularis Sinicae*, 1st ed.; Science Press: Beijing, China, 1984; Volume 53, pp. 154–155.
9. Yoshida, T.; Arioka, H.; Fujita, T.; Chen, X.M.; Okuda, T. Monomeric and dimeric hydrolysable tannins from two melastomataceous species. *Phytochemistry* **1994**, *37*, 863–866. [CrossRef]
10. Zou, J.M.; Zhong, X.Q.; Lu, G.R. *Selection and Compilation of Characteristic Chinese Herbal Medicine Resources in Guangxi*, 1st ed.; Science Press: Beijing, China, 2011; pp. 273–274.
11. Tang, T.X.; Zheng, H.; Liu, Y.; Qiu, X.H. Determination of water extracts of *Melastoma candidum* and *Melastoma normale* by HPLC-DAD-ESI-MS/MS. *Strait Pharm. J.* **2016**, *28*, 46–48.
12. Nonaka, G.I.; Ishimaru, K.; Mihashn, K.; Iwase, Y.; Ageta, M.; Nishioka, T.; Nishioka, I. Tannins and related compounds. lxiii.: Isolation and characterization of mongolicains A and B, novel tannins from *quercus* and *castanopsis* species. *Chem. Pharm. Bull.* **1988**, *36*, 857–869. [CrossRef]
13. Chen, S.J.; Huang, Y.Z.; Jian, L.U.; Liu, J.Q.; Huang, H.L.; Shu, J.C. Phenolic components from roots of *Psidium guajava*. *Chin. J. Exp. Trad. Med. Formulae* **2019**, *25*, 169–174.
14. Min, B.S.; Tomiyama, M.; Ma, C.M.; Nakamura, N.; Hattori, M. Kaempferol acetylrhamnosides from the rhizome of *Dryopteris crassirhizoma* and their inhibitory effects on three different activities of human immunodeficiency virus-1 reverse transcriptase. *Chem. Pharm. Bull.* **2001**, *49*, 546–550. [CrossRef]
15. Wang, G.J.; Tsai, T.H.; Lin, L.C. Prenylflavonol, acylated flavonol glycosides and related compounds from *Epimedium sagittatum*. *Phytochemistry* **2007**, *68*, 2455–2464. [CrossRef]
16. Zhang, L.; Gao, H.Y.; Baba, M.; Okada, Y.; Okuyama, T.; Wu, L.J.; Zhan, L.B. Extracts and compounds with anti-diabetic complications and anti-cancer activity from *Castanea mollissina* Blume (Chinese chestnut). *BMC Complem. Altern. Med.* **2014**, *14*, 422. [CrossRef]
17. Cheng, Y.X.; Zhou, J.; Tan, N.H. The chemical constituents of *Parakmeria yunnanensis*. *Acta Bot. Yunnanica* **2001**, *23*, 352–356.
18. Zhong, X.N.; Otsuka, H.; Ide, T.; Hirata, E.; Takushi, A.; Takeda, Y. Three flavonol glycosides from leaves of *Myrsine seguinii*. *Phytochemistry* **1997**, *46*, 943–946. [CrossRef]
19. Samy, M.N.; Sugimoto, S.; Matsunami, K.; Otsuka, H.; Kamel, M.S. One new flavonoid xyloside and one new natural triterpene rhamnoside from the leaves of *Syzygium grande*. *Phytochem. Lett.* **2014**, *10*, 86–90. [CrossRef]
20. He, R.J.; Wang, Y.F.; Li, D.P.; Huang, Y.L. Phenolic constituents from Melastoma normale. *Guihaia* **2020**, *40*, 641–647.
21. Takashi, T.; Nobuko, U.; Hideo, S.; Gen-Ichiro, N.; Isao, K. Four new-C-glycosidic ellagitannins, castacrenins D-G, from japanese chestnut wood (*Castanea crenata* SIEB. et ZUCC.). *Chem. Pharm. Bull.* **1997**, *45*, 1751–1755. [CrossRef]
22. Yoshida, T.; Hatano, T.; Kuwajima, T.; Okuda, T. Oligomeric hydrolyzable tannins. Their ^{1}H NMR spectra and partial degradation. *Heterocycles* **1992**, *33*, 463–482.
23. Fujieda, M.; Tanaka, T.; Suwa, Y.; Koshimizu, S.; Kouno, I. Isolation and structure of whiskey polyphenols produced by oxidation of oak wood ellagitannins. *J. Agric. Food Chem.* **2008**, *56*, 7305–7310. [CrossRef] [PubMed]
24. Okuda, T.; Yoshida, T.; Hatano, T. Circular dichroism of hydrolysable tannins-I ellagitannins and gallotannins. *Tetrahedron Lett.* **1982**, *23*, 3937–3940. [CrossRef]
25. Okuda, T.; Yoshida, T.; Hatano, T. New methods of analyzing tannins. *J. Nat. Prod.* **1989**, *52*, 1–31. [CrossRef]
26. Rho, H.S.; Ghimeray, A.K.; Yoo, D.S.; Ahn, S.M.; Cho, J.Y. Kaempferol and kaempferol rhamnosides with depigmenting and anti-inflammatory properties. *Molecules* **2011**, *16*, 3338–3344. [CrossRef] [PubMed]
27. Wang, L.; Wang, B.; Li, H.; Lu, H.C.; Qiu, F.; Xiong, L.; Xu, Y.H.; Wang, G.M.; Liu, X.L.; Wu, H.W. Quercetin, a flavonoid with anti-inflammatory activity, suppresses the development of abdominal aortic aneurysms in mice. *Eur. J. Pharm.* **2012**, *690*, 133–141. [CrossRef] [PubMed]
28. Kim, H.H.; Kim, D.H.; Kim, M.H.; Oh, M.H.; Kim, S.R.; Park, K.J.; Lee, M.W. Flavonoid constituents in the leaves of *Myrica rubra* sieb. et zucc. with anti-inflammatory activity. *Arch. Pharm. Res.* **2013**, *36*, 1533–1540. [CrossRef]
29. Cheng, H.L.; Zhang, L.J.; Liang, Y.H.; Hsu, Y.W.; Lee, I.J.; Liaw, C.C. Antiinflammatory and antioxidant flavonoids and phenols from *Cardiospermum halicacabum*. *J. Trad. Comp. Med.* **2013**, *3*, 33.
30. Fan, M.; Zhang, G.; Hu, X.; Xu, X.; Gong, D. Quercetin as a tyrosinase inhibitor: Inhibitory activity, conformational change and mechanism. *Food Res. Int.* **2017**, *100*, 226–233. [CrossRef]
31. Kishore, N.; Twilley, D.; Analike, B.; Verma, P.; Singh, B.; Cardinali, G. Isolation of flavonoids and flavonoid glycosides from myrsine africana and their inhibitory activities against mushroom tyrosinase. *J. Nat. Prod.* **2018**, *81*, 49–56. [CrossRef]